Article

Preparation of a Novel Straw−Sludge Activated Biochar and Its Adsorption Mechanisms for Removal of VOCs

Xiaohui Pan, Ninglu Zhang, Le Yang, Chao He, Xiaoran Ma, Xinxin Liu, Liang Liu, Tingting Hou, and Youzhou Jiao*

Cite This: ACS Omega 2023, 8, 39329−39344

Read Online

ACCESS | Metrics & More | Article Recommendations

ABSTRACT: To simultaneously achieve the objectives of waste resource utilization and clean production, a novel approach involving the utilization of corn straw−sludge hybrid biochar was proposed for the adsorption of VOCs emitted from biomass power plants. This study analyzed the effect of straw−sludge biochar on the adsorption characteristics of VOCs (toluene, isopentane, and ethylene) under different preparation conditions (raw material ratio, activation temperature, and activation time). The findings revealed that the adsorption efficiency of the mixed biochar was significantly superior to that of individual corn straw biochar and sludge biochar. The adsorption of methylbenzene, isopentane, and ethylene was 78.32, 40.81, and 41.18% higher, respectively, compared to the control groups consisting of pure sludge biochar and pure corn straw biochar. Moreover, the adsorption performance of the activated biochar followed the sequence of ethylene < isopentane < methylbenzene in terms of both saturation time and adsorption capacity. The adsorption capacity of VOCs on straw biochar−sludge biochar demonstrated a consistent correlation with the boiling point and molecular weight of the adsorbate, with higher adsorption capacities observed for adsorbates with larger boiling points and molecular weights, specifically methylbenzene > isopentane > ethylene.
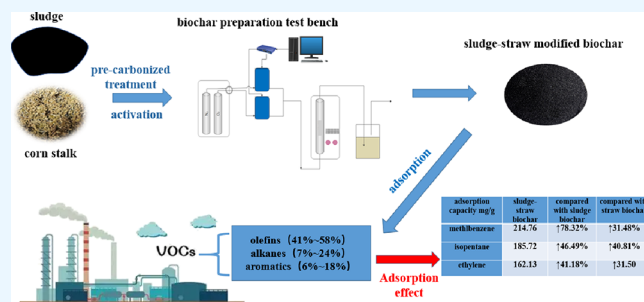
1. INTRODUCTION

The utilization of biomass energy offers a viable solution for optimizing the energy structure, reducing CO_2 emissions, safeguarding the ecological environment, and addressing climate change.[1] Sludge and crop straw are significant examples of waste biomass resources. By employing pyrolysis technology, the cotreatment of sludge and crop straw can harness their distinctive properties, enabling the realization of their individual values and the exploitation of their complementary advantages. This approach has emerged as a prominent focus in the treatment of sewage sludge and crop straw. Copyrolysis of sludge and straw to generate biochar not only eliminates bacteria, pathogens, and other toxic substances in the sludge but also stabilizes harmful heavy metals within the biochar matrix.[2,3] Additionally, the presence of crop straw during the carbonization process facilitates moisture adjustment, while the alkali metals present in crop straw serve as catalysts in the copyrolysis process.[4,5] The resulting product, straw−sludge biochar, exhibits a large specific surface area and well-developed pore structure, rendering it capable of adsorbing organic pollutants from the environment and facilitating environmental remediation.[6]

Due to the distinct characteristics of biomass fuel combustion in comparison to coal combustion, the combus-tion byproducts of biomass, with the exception of SO_2 and NO_x, contain a substantial amount of volatile organic compounds (VOCs), constituting approximately 10% of the emissions.[7] Presently, research on flue gas purification technologies for biomass fuel boilers predominantly focuses on conventional coal-fired boiler flue gas purification methods, with an emphasis on particle and SO_2 removal, while VOC purification, as well as NO_x removal, has received less attention. As environmental protection standards continue to advance, there is an urgent need to develop cost-effective and operationally simple technologies for treating VOCs in flue gas emitted by biomass boilers. The application of biochar as an adsorbent for capturing flue gas VOCs from biomass power plants presents an effective approach to mitigate issues such as the corrosion of boiler pipes caused by chemical additives and the high cost associated with chemical activators.[8] In light of the challenges associated with waste resource utilization and

the absence of VOC-removal technology in biomass power plants, the utilization of a combination of slip-and-straw biochar presents an opportunity for VOC removal in these plants. This approach not only allows for waste recycling and resolution of associated environmental pollution issues but also expands the current understanding of VOC emission reduction in biomass power plants. Alagu et al. conducted a study on the emission characteristics of industrial biomass fuel power plants, revealing that the emitted VOCs were predominantly composed of olefins, alkanes, and aromatics, which collectively accounted for over 85% of the total VOCs.[9] Specifically, ethylene was the primary olefin, *n*-isopentane was the main alkane, and methylbenzene was the major aromatic compound. Therefore, investigating the adsorption of ethylene, methylbenzene, and isopentane by biochar serves as a theoretical foundation for VOC emission reduction technology.

The carbon source of traditional biochar usually comes from coal, asphalt, and some other nonrenewable resources, so the cost is relatively high. In recent years, biochar has attracted more and more attention due to its low cost and renewable advantages. Activated biochar based on biochar synthesis has been gradually used in wastewater treatment, hydrogen storage, supercapacitors, and other applications.[10−13] There have been some reports on the application of biochar in VOC adsorption, Zhang, et al., Ukalska-Jaruga et al., and Akinpelu et al. explored biochar's adsorption capacity for VOCs. They have enhanced the adsorption performance for methylbenzene and benzene by modifying the surface functional groups and structures of activated biochar. Furthermore, they examined the adsorption behavior of aromatic hydrocarbons on activated carbon with different pore structures, noting that the adsorption process was influenced by the molecular polarity and structure of the adsorbed compounds. The presence of polar substituents decreased the adsorption of methylbenzene on activated carbon.[14−16] Khan et al., Zhang et al., Shih et al., and others studied the impact of activated biochar on the adsorption of propylene, butene, and 1-pentene. They found that physical adsorption in micropores and mesoporous pores was the primary mechanism for olefin adsorption by activated biochar. Activated biochar with higher pore volume exhibited more favorable adsorption properties.[17−19] The research conducted by Yang et al., Hou et al., Chanchez-Monedero et al., and others involved modifying the surface structure and functional groups of activated biochar through physical and chemical activation. They discovered that increasing the specific surface area and pore volume as well as reducing oxygen-containing groups on the surface facilitated the adsorption of methane, *n*-butane, and cyclohexane. Additionally, reducing acid oxygen-containing functional groups and hydrophilic groups on the surface of activated biochar enhanced its adsorption capacity for alkanes.[20−22]

In summary, most of the current studies on the adsorption of VOCs by biochar choose biochar prepared from a single raw material and the activation methods are mostly redox modification or loading modification. Although this activation method enhances the interaction between the surface of the material and the target adsorption molecules, it is costly and has the risk of environmental pollution. However, biochar prepared by physical activation (CO_2 or H_2O) can avoid these shortcomings, and there are few related studies. In addition, at present, research on VOC emission reduction technology in biomass power plants based on biochar adsorption has not been reported. Finally, in the related research on VOC

adsorption by biochar, the adsorbate is also mostly single-phase VOCs with no competitive relationship, and there are few reports discussing the competitive relationship of multiphase VOCs. In this research, sludge and corn straw, both biomass raw materials, were utilized to prepare straw−sludge biochar using CO_2 as the activating agent. The aim was to investigate the adsorption efficiency of mixed biochar on VOCs (methylbenzene, isopentane, and ethylene) generated from biomass power plant combustion. Furthermore, the study explored the adsorption performance of straw−sludge biochar under varying proportions of raw materials, the activation temperature, and the activation time. By analysis of the isothermal adsorption curve, penetration curve, and adsorption kinetics, the optimal preparation conditions for mixed biochar, which demonstrated effective synergy in VOCs removal, were determined. These findings establish a theoretical basis for VOC removal from biomass combustion flue gas and contribute to the advancement of biomass clean combustion technology.

2. EXPERIMENTAL SECTION

2.1. Experimental Materials. The sludge used in this study was obtained from Zhengzhou Matougang Sewage Plant and underwent a natural air-drying process for 7 days. Subsequently, it was subjected to constant temperature drying in an oven at 105 °C until the quality remained unchanged. The dried sludge was then crushed and screened using a 100 mesh stainless steel screen. The corn straw was sourced from the experimental farmlands of Henan Agricultural University. It was washed with distilled water 3 times, followed by constant temperature drying in an oven at 105 °C until the quality stabilized. The dried corn straw was then crushed and screened using a 100 mesh stainless steel screen. Standard gas cylinders containing 100 ppm of methylbenzene/nitrogen, isopentane/nitrogen, and ethylene/nitrogen gases were obtained from Jining Xieli Special Gas Co., Ltd. The experimental setup consisted of a standard gas unit, adsorption unit, and data monitoring unit. The system included a gas pressure-reducing valve, a gas mass flow meter, and polytetrafluoroethylene piping, which exhibited excellent chemical stability. Figure 1 illustrates the experimental configuration for biochar preparation and VOC adsorption.

2.2. Experimental Method. The optimal carbonization conditions were determined by selecting the raw material proportion (sludge-to-corn straw ratio), activation temperature, and activation time. The sludge and corn straw were mixed and placed in a tube furnace under a nitrogen atmosphere. The temperature was increased at a rate of 10 °C/min until it reached 600 °C, and the material was held at this temperature for 120 min. Afterward, the mixture was cooled to room temperature to obtain the carbonized material. The carbonized material passed through a 100 mesh screen was used as the activation raw material. The activation process involved injecting nitrogen into the furnace during the heating stage, switching to CO_2 gas for activation, and then stopping the heating. The activated gas was purged with nitrogen and cooled to room temperature, resulting in the formation of a straw−sludge biochar.

To achieve the desired concentration of VOCs, the gas flow was controlled. The standard gas bottle and nitrogen bottle were adjusted to 0.1 MPa by using a pressure-reducing valve, and the gas mass flow meter was calibrated. An online VOC detector was used to monitor the outlet concentration,

(a)

(b)
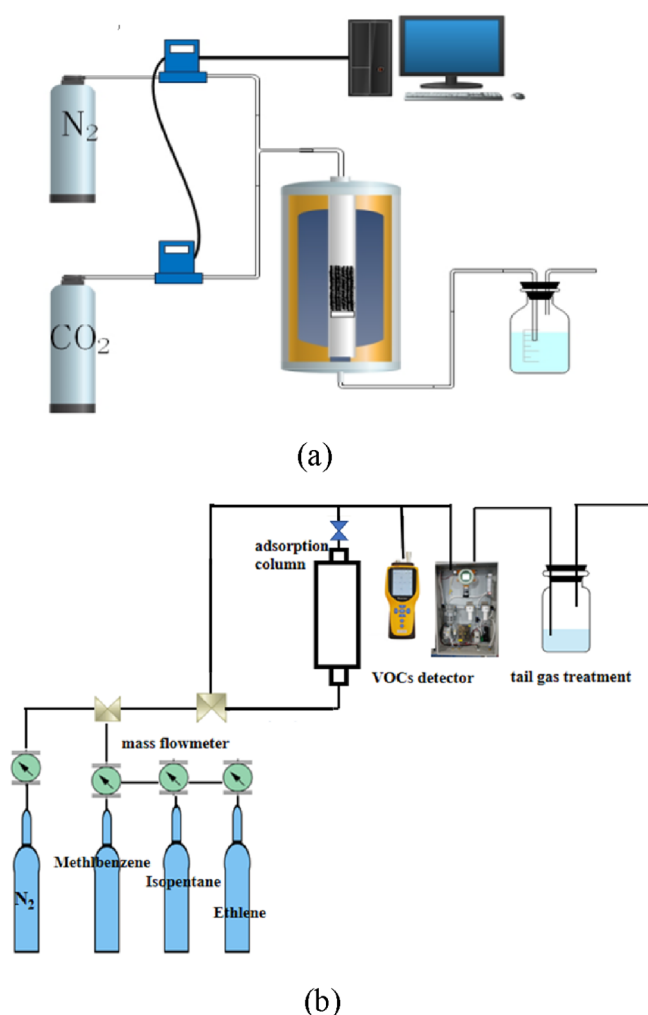
Figure 1. Experimental device diagrams: (a) preparation of the biochar experimental equipment diagram and (b) diagram of the experimental device for adsorption of VOCs.

ensuring that it stabilized at the desired level before the experiment. The adsorption column, made of glass, measured 20 cm in length and 2 cm in diameter and was maintained at an adsorption temperature of 25 °C. The inlet and outlet concentrations were measured using an online VOC detector. Each adsorption experiment involved using 1.5 g of biochar as the adsorbent and a gas volume of 500 mL/min as the inlet flow rate. Adsorption saturation was reached when the outlet concentration equaled the inlet concentration. For single VOC adsorption experiments, the biochar adsorbent was placed in the adsorption column and the corresponding VOCs standard gas was introduced while monitoring the gas concentration with the online VOC detector. The experiment concluded when the outlet concentration equaled the inlet concentration, at which point, the adsorbent was replacedwith the next sample. This process was repeated for successive adsorption experiments. For binary adsorption experiments, methylbenzene—isopentane, methylbenzene—ethylene, and isopentane—ethylene mixtures at different concentration ratios (1:6, 1:1, and 6:1) were passed through the adsorption column. The sampling and detection method remained the same as in the single adsorption tests using two detectors and adjusting the conversion coefficient for the respective gases under test. The desired concentrations of methylbenzene, isopentane, or

ethylene were adjusted and confirmed for accuracy before real-time observation and recording of the detector values. After the experiment, the gas cylinder was closed.

2.3. Test Method. The specific surface, pore volume, and pore size of the samples were calculated by N_2 adsorption at a relative pressure of 0.1−1 and a temperature of 77 K for liquid nitrogen. The Brunauer−Emmett−Teller (BET) method was used to compare surface area data, and the Barret-Joyner-Halenda (BJH) tnechnique was employed to determine pore size. The pretreatment method was 5 h of vacuum degassing at 200 °C. The functional groups of biochar were tested using a Fourier transform infrared spectrometer and potassium bromide pellet method. The test requirements were that the scanning range was 400−4000 cm^{-1}, and the number of scanning was 32 times. The surface morphology of the samples was analyzed by a Zeiss Sigma 300 scanning electron microscope (SEM) at room temperature.

2.4. Experimental Design of the Response Surface Method. Based on preliminary experiments, three key factors (raw material ratio, activation temperature, and activation time) that significantly impact VOC adsorption were selected. The response surface method was then employed to optimize these factors and determine the optimal conditions for preparing straw−sludge biochar. The adsorption quantities of methylbenzene, isopentane, and ethylene were used as the response values in the experimental design. The factors and levels used in the experiments are detailed in Tables 1 and 2,

Table 1. Factors and Levels of Response Surface Analysis

independent variable	symbol	code number		
		−1	0	1
raw material ratio	A	0.25	0.50	0.75
activation temperature (°C)	B	700	800	900
activation time (min)	C	60	120	180

and the corresponding labels are explained in Table 3. Using Design Expert software, a test scheme was designed and the results were analyzed. Regression analysis was performed on the experimental data to establish and validate the regression equation. Finally, the optimal process parameters for preparing

Table 2. Response Surface Test Design

experiment number	A—raw material ratio	B—activation temperature (°C)	C—activation time (min)
1	0.50	800	120
2	0.50	800	120
3	0.50	800	120
4	0.50	800	120
5	0.50	800	120
6	0.50	700	60
7	0.50	900	60
8	0.50	900	180
9	0.50	700	180
10	0.75	800	60
11	0.75	900	120
12	0.75	800	180
13	0.75	700	120
14	0.25	800	60
15	0.25	800	180
16	0.25	900	120
17	0.25	700	120

Table 3. Label Description

symbol	explain
AC	active biochar
MAC	response surface group straw−sludge biochar
SAC	sludge biochar
CAC	corn straw biochar
OAC	straw−sludge biochar with the optimal adsorption effect
BC	biomass biochar
-C	CO_2 activation
M	methylbenzene
I	isopentane
E	ethylene
MAC-1−17	response surface straw−sludge biochar prepared by 17 groups of experiments
MAC-C-1−17	straw−sludge biochar prepared by 17 groups of CO_2 activation response surface experiments
OACM	straw−sludge biochar with the optimal methylbenzene adsorption effect
OACI	straw−sludge biochar with the optimal isopentane adsorption effect
OACE	straw−sludge biochar with the optimal ethylene adsorption effect

straw−sludge biochar were obtained based on the regression equation.[23]

2.5. Kinetic Analysis. The investigation of adsorption kinetics allows us to determine the rate at which methylbenzene, isopentane, and ethylene are adsorbed by biochar and provides insights into the underlying adsorption mechanism.[24]

The adsorption kinetic curve in this study was fitted using a quasi-first-order kinetic model and quasi-second-order kinetic model. The quasi-first-order and quasi-second-order kinetic models are shown in eqs 1 and 2 below.

$$\ln(q_e - q_t) = \ln q_e - k_1 t \tag{1}$$

$$\frac{t}{q_t} = \frac{1}{k_2 q_e^2} + \frac{t}{q_e} \tag{2}$$

where k_1 (min^{-1}) and k_2 [(g.mg)$^{-1}$.min^{-1}] are the adsorption rate constants; q_e (mg/g) and q_t (the Langmuir model) are the adsorption capacities at adsorption equilibrium and reaction time t, respectively.

2.6. Adsorption Isotherm. The Langmuir model is suitable for describing the equilibrium adsorption behavior of methylbenzene, isopentane, and ethylene on biochar. The Langmuir equation assumes monolayer adsorption where each adsorption site is independent, and the surface is uniform.[25] The Freundlich model is suitable for multilayer adsorption in which the physical and chemical properties of the adsorbent surface are heterogeneous. The Langmuir model and Freundlich model are shown in eqs 3 and 4.

$$\frac{\rho_e}{q_e} = \frac{\rho_e}{q_m} + \frac{1}{k_L q_m} \tag{3}$$

$$\ln q_e = \ln k_F + \frac{\ln \rho_e}{n} \tag{4}$$

where q_e and ρ_e denote the adsorption capacity (mg/g) and the intake concentration (mg/m^3) at adsorption equilibrium, respectively. q_m denotes the theoretical maximum adsorption capacity (mg/g), k_L is the Langmuir adsorption rate constant (L/mg), k_F is the Freundlich adsorption rate constant (mg·g^{-1}·(L·mg-1)$^{-1/n}$), and n is the adsorption strength.

3. RESULTS AND DISCUSSION

3.1. Characterization of Straw−Sludge Biochar. *3.1.1. Analyses of the Specific Surface Area and Pore Structure.* The adsorption performance of biochar is significantly affected by its specific surface area and pore structure. The nitrogen adsorption−desorption isotherm curve and pore structure distribution of biochar are shown in Figure 2. It can be seen from Figure 2a that the adsorption isotherm curve of unactivated biochar (BC) is type I, and hysteresis loops appear on the adsorption and desorption isotherm curve of CO_2-activated biochar (OAC), which belongs to a type-IV adsorption isotherm phenomenon. The gas adsorption capacity rises sharply to the limit with the increase of pressure under low pressure. The hysteresis loops formed by the two smooth curves are generated under high pressure, indicating that the pore structure of OAC is mainly microporous and the adsorption capacity is good. As can be seen from Figure 2b, the pore size distribution of the prepared biochar is 0−6 nm, most of which are below 5 nm, about 80% of which are micropores, and only 20% are mesopores, without macropores. The pore structure distribution diagram shows that micropores and mesopores coexist in activated/unactivated biochar and are mainly composed of micropores, which belong to the structure
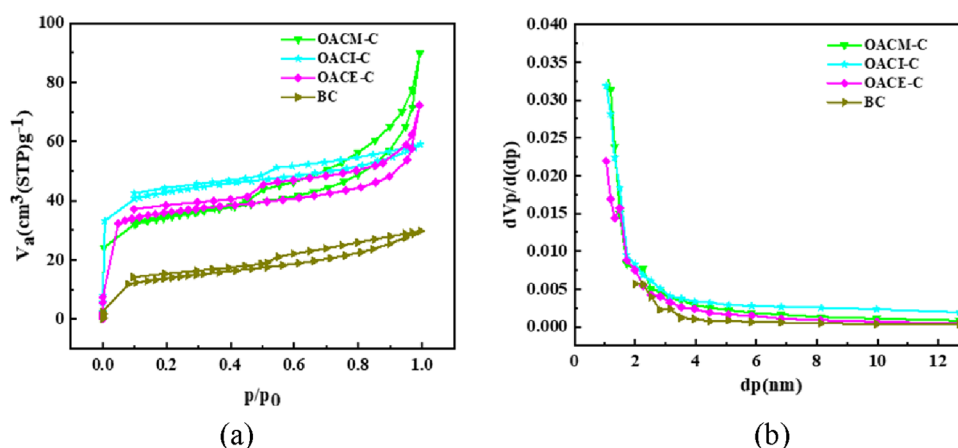
Figure 2. Nitrogen adsorption−desorption isotherm and pore structure distribution. (a) Nitrogen adsorption−desorption isotherm curve. (b) Pore structure distribution curve.

of micropores and mesopores mixing, and this pore structure is conducive to the adsorption of biochar molecules with different sizes.

Table 4 shows the specific surface area, pore volume, and pore diameter of biochar. The experimental data showed that

Table 4. Specific Surface Area, Pore Volume, and Average Pore Size of Average Pore Diameter

adsorbent	specific surface area (m^2/g)	pore volume (cm^3/g)	average pore diameter (nm)
SAC	68.15	0.0659	5.2034
CAC	63.64	0.0691	5.9349
OACM-C	125.17	0.1229	3.7634
OACI-C	110.19	0.1118	4.0067
OACE-C	123.75	0.1227	3.6566
BC	45.29	0.0456	7.0577

the maximum specific surface area of MAC-C-1−17 was 119.25m^2/g, the pore volume was 0.0668−0.1263 cm^3/g, and the average pore size was 3.2083−5.5508 nm. Table 4 shows that the order of specific surface area is OAC-C > SAC > CAC > BC. The specific surface areas of straw−sludge biochar activated by CO$_2$ was 83.67 and 96.68% higher than that of pure sludge and pure corn straw biochar, respectively. The specific surface area of activated biochar was larger than that of unactivated biochar, and the average pore size of activated biochar was lower than that of unactivated biochar. The results showed that, when the biochar was activated by CO$_2$, some organic matter escaped, the pore structure opened, the pore structure became richer, the pore volume and specific surface area increased, and the average pore size became smaller. The increase of specific surface area is conducive to the exposure of adsorption sites, and the large specific surface area and appropriate mesoporous are conducive to the transport and diffusion of ions in biochar.[26]

3.1.2. Functional Group. The Fourier transform infrared spectra of biochar are shown in Figure 3. The peaks are
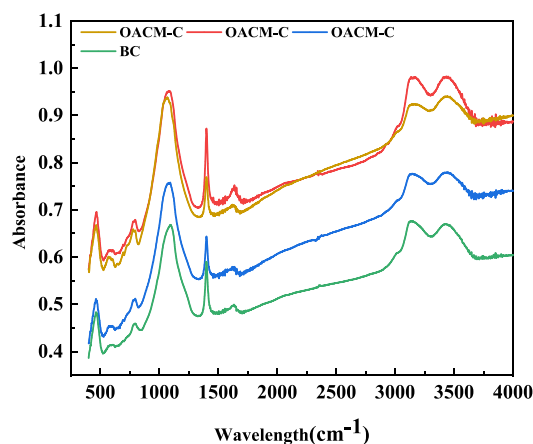
Figure 3. Fourier transform infrared spectra of biochar.

concentrated near 470 cm^{-1} (P−O), 790 cm^{-1} (N−O), 1110 cm^{-1} (C−O−C), 1400 cm^{-1} (C−O), 1630 cm^{-1} (C=C), and 3200 and 3448 cm^{-1} (−OH). The four groups of samples have similar peak shapes, but the peak values are slightly different, indicating that the types of functional groups on the surface of activated modified biochar do not change significantly. The surface functional groups of the four groups of sludge-based

biochar contain N−O, C−O−C, C=C, and −OH functional groups, and the types of functional groups are roughly the same. There are functional groups, such as hydroxyl and carboxyl groups, on the surface and inside of the OAC to complexate with the surface of biochar, and the oxygen functional groups on the surface are related to the adsorption process of VOCs.

3.1.3. SEM Analysis. The SEM images of biochar are shown in Figure 4. Figure 4d shows that, compared with activated biochar, the surface of unactivated biochar is relatively flat, slightly rough, and has irregular pore structure, but the pore structure is relatively shallow. This is due to the hydrolysis of some functional groups in sludge and corn straw during carbonization, and the different oxidation degree leads to different pore forms. Figure 4a−c is the scanning electron microscope images of activated biochar. Compared with the biochar before activation, its surface is rougher, showing dense and irregular lines, more dense pore structure, and deep surface pores. This is because the high-temperature pyrolysis is realized under the catalysis of CO$_2$ gas activation, which makes some small pores appear on the inner wall of activated biochar pores, and increases the proportion of micropores and mesopores.

3.2. Study on Adsorption Characteristics of Straw−Sludge Biochar Prepared by the CO$_2$ Activation Method. *3.2.1. Penetration Curve.* When the adsorbate enters the adsorption column, the adsorbate gas flow contacts the biochar, and the adsorbate molecules are quickly adsorbed on the biochar. At this time, the gas flow from the outlet of the adsorption column contains almost no adsorbate molecules. With an increasing amount of adsorbate entering the adsorption column, the adsorbate molecules finally break through the adsorption column. The time required for this process is called penetration time. Figure 5 displays the dynamic adsorption and penetration curves of biochar for VOCs (methylbenzene, isopentane, and ethylene). Figure 5a−c presents the adsorption penetration curves of straw−sludge biochar, pure sludge biochar, and pure corn straw biochar in response surface groups, while Figure 5d illustrates the adsorption penetration curves of the optimal response surface group and unactivated biochar. The adsorption penetration curves of biochar for methylbenzene, isopentane, and ethylene follow a similar S-shaped trend, exhibiting significant variations with changes in the biochar.

In Figure 5a, the adsorption and penetration time of pure sludge biochar (SAC-C) for methylbenzene are the shortest, 35 min, indicating the lowest adsorption effectiveness. The majority of response surface groups showed an adsorption and penetration time of 50 min for straw−sludge biochar. Pure corn straw biochar (CAC-C) exhibits an adsorption and penetration time of 45 min for methylbenzene, longer than those of response surface groups MAC-C-12, MAC-C-13, and MAC-C-16 but shorter than those of the other 14 groups. Figure 5b shows that the adsorption and penetration time of isopentane for pure sludge biochar (SAC-C) are 35 min, identical to those of MAC-C-14 and MAC-C-17 and shorter than those of other response surface groups and pure corn straw biochar. Pure corn straw biochar (CAC-C) has an adsorption and penetration time of 50 min for isopentane, which is longer than those of MAC-C-9, MAC-C-14, and MAC-C-17 in the response surface group but equal to or shorter than that of straw−sludge biochar in the other 14 response surface groups. In Figure 5c, the adsorption and

(a)

(b)

(c)

(d)
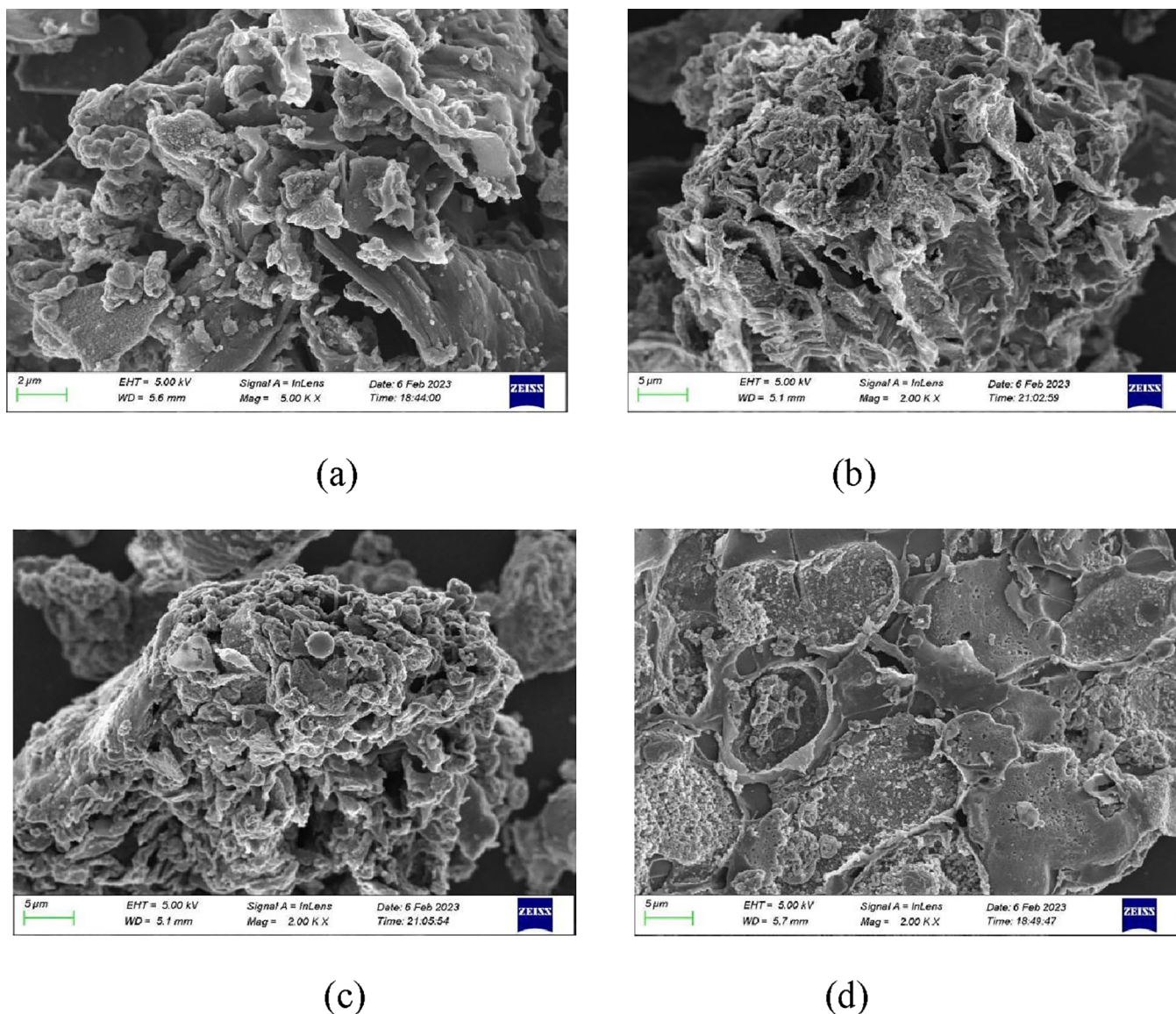
Figure 4. SEM of straw−sludge biochar: (a) OACM-C, (b) OACI-C, (c) OACE-C, and (d) BC.

penetration time of ethylene for pure sludge biochar (SAC-C) and pure corn straw biochar (CAC-C) is 40 min, which is lower than the 45 or 50 min adsorption and penetration time of ethylene for straw−sludge biochar in response surface groups MAC-C-1 to MAC-C-17. In Figure 5d, the adsorption penetration times of methylbenzene, isopentane, and ethylene for the optimal group of straw−sludge biochar (OAC-C) obtained from response surface analysis are 50, 40, and 30 min with saturation times of 110, 120, and 120 min, respectively. Unactivated straw−sludge biochar (BC) shows an adsorption and penetration time of 5 min for methylbenzene, isopentane, and ethylene, with saturation times of 55, 35, and 30 min. CO_2 activation extends the penetration time by 25−45 min and the adsorption saturation time by 55−90 min, thereby improving the utilization rate of straw−sludge biochar. Generally, a longer penetration time indicates a better dynamic adsorption capacity of straw−sludge biochar under the same adsorption conditions. The rapid rise of the adsorption curve after penetration suggests a small mass transfer resistance in the adsorption column and a high adsorption rate. The adsorption capacity of the optimal group of straw−sludge biochar follows

the order of OACM-C > OACI-C > OACE-C. The penetration time and saturation adsorption time of CO_2-activated straw−sludge biochar are longer than those of unactivated biochar. The penetration curves of CO_2-activated straw−sludge biochar demonstrate highly efficient adsorption of methylbenzene, isopentane, and ethylene before penetration, with a decrease in adsorption capacity after penetration until saturation adsorption is reached. The adsorption performance of CO_2-activated straw−sludge biochar is improved compared to that of unactivated biochar. Activation increases the specific surface area and improves the pore structure of straw−sludge biochar, thereby reducing diffusion resistance for methylbenzene, isopentane, and ethylene in the pores and facilitating their diffusion in the straw−sludge biochar adsorption column.

3.2.2. Adsorption Curve. Figure 6 illustrates the adsorption curves of biochar on VOCs. Figure 6a−c displays the variation in adsorption capacity over time for 17 groups of straw−sludge biochar, pure sludge biochar, and pure corn straw biochar, respectively, on the response surface. Figure 6d depicts the
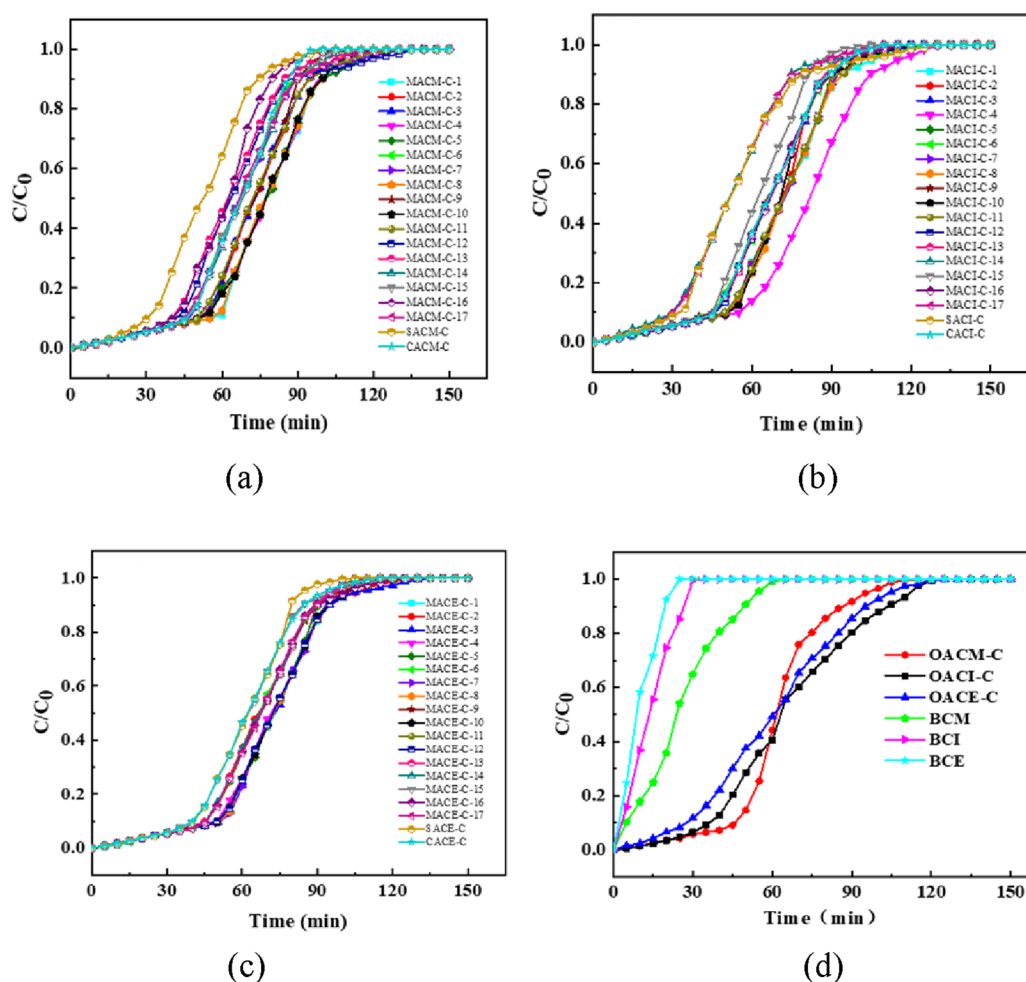
Figure 5. Penetration curves of biochar on VOCs (biochar 1.5 g, VOCs 100 ppm): (a) methylbenzene, (b) isopentane, (c) ethylene, and (d) optimal group and inactive group.

adsorption curves of the response surface optimal group of straw—sludge biochar and unactivated biochar.

Upon comparison and analysis of the adsorption effects of straw—sludge biochar under different preparation conditions after CO_2 activation, it can be concluded that the adsorption of VOCs increases with the extension of adsorption time. As observed in the figure, the early stage of adsorption for straw—sludge biochar exhibits a rapid adsorption phase lasting 40 min, followed by a gradual decrease in the adsorption rate. Initially, VOCs rapidly disperse within the pores of straw—sludge biochar upon contact, occupying numerous adsorption sites. However, over time, the available adsorption sites decrease. Among the adsorption of methylbenzene, isopentane, and ethylene by straw—sludge biochar, the MAC-1 to MAC-5 groups demonstrate the highest adsorption capacity, ranging from 210.15 to 214.04 mg/g, from 178.26 to 182.05 mg/g, and from 162.25 to 166.59 mg/g, respectively. Saturation results are reached at 100, 105, and 95 min, respectively, with the fastest increase in adsorption capacity occurring within the first 40 min.

From Figure 6a, it is evident that the adsorption capacity of pure sludge biochar (SACM) is the lowest throughout the entire adsorption process of methylbenzene. The adsorption capacity of pure corn straw biochar (CACM) is higher than those of MACM-16, MACM-17, and CACM-19 but lower than those of MACM-1 to MACM-15 groups. Figure 6b

reveals that SACI of pure sludge biochar exhibits a higher adsorption capacity than MACI-17 but lower than MACI-1 to MACI-16 and pure corn straw biochar (CACI) groups during the adsorption process of isopentane. Additionally, CACI of pure corn straw biochar displays higher adsorption capacity than MACI-14, SACI, MACI-17, and lower than other groups. Figure 6c demonstrates that, during the adsorption process of ethylene, the adsorption capacity of pure sludge biochar (SACE) is the lowest, followed by pure corn straw biochar (CACE). As the adsorption time increases, the adsorption capacity of ACE-1 to ACE-17 in the experimental group surpasses that of the single control group. The adsorption capacity of VOCs in biochar prepared by mixing sludge with corn straw is significantly higher than that of biochar prepared from a single raw material. Mixed biochar exhibits an enhanced capability for VOCs to enter the pores and undergo adsorption. Figure 6 reveals significant variations in the adsorption capacity of CO_2-activated straw—sludge biochar, with the optimal group (OACM-C, OACI-C, and OACE-C) exhibiting adsorption capacities of 214.76 185.72, and 162.13 mg/g for VOCs, respectively. Additionally, the adsorption capacity of unactivated biochar follows the sequence of methylbenzene > isopentane > ethylene, with adsorption amounts of 23.62, 18.57, and 15.48 mg/g, respectively.

The adsorption capacity values of CO_2-activated straw—sludge biochar are 9.09, 10, and 10.47 times higher than those
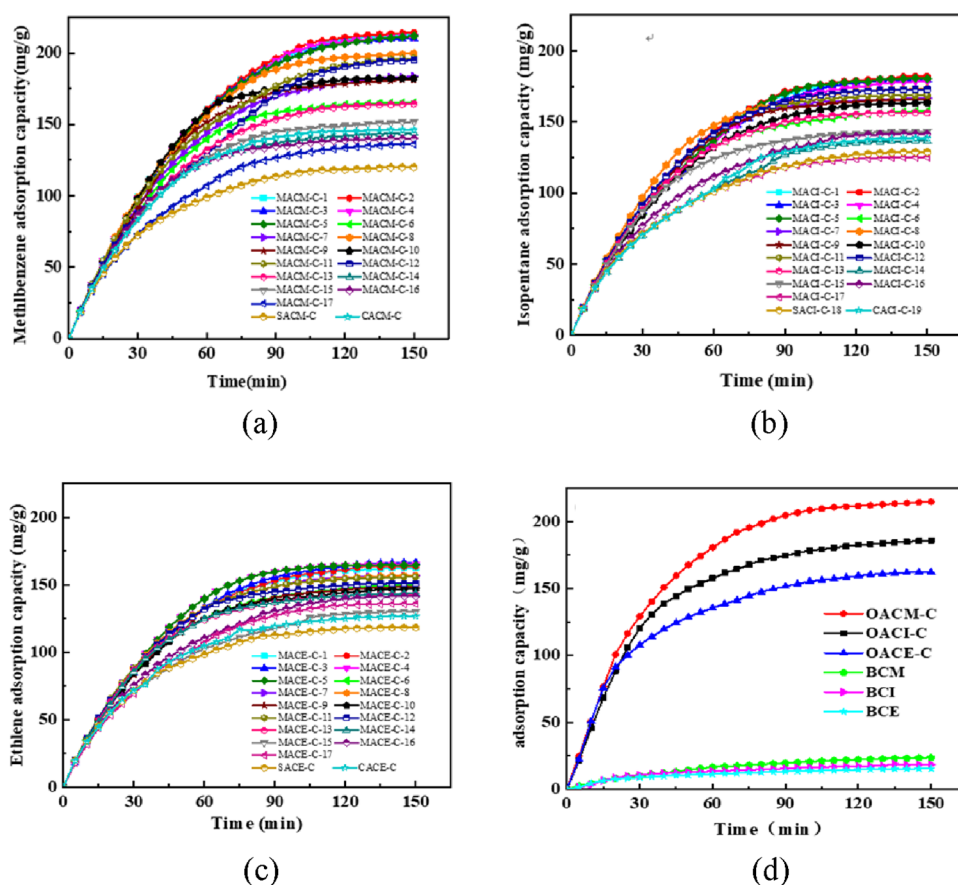
Figure 6. Adsorption curves of biochar on VOCs ((biochar 1.5 g, VOCs 100 ppm): (a) methylbenzene, (b) isopentane, (c) ethylene, and (d) the optimal group and inactive group
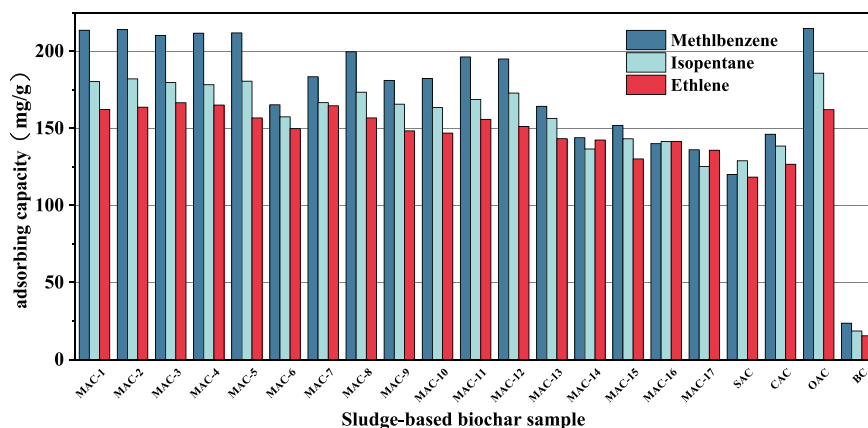
Figure 7. Adsorption capacities of activated carbon samples for VOCs

of unactivated straw—sludge biochar for methylbenzene, isopentane, and ethylene, respectively. This improvement can be attributed to the larger pore size and specific surface area of CO_2-activated straw—sludge biochar, facilitating the diffusion of VOC molecules into the micro- and macropores of the biochar, enhancing adsorption reactions.[27]

3.2.3. Saturation Adsorption Capacity. Figure 7 displays the saturation adsorption capacity values of methylbenzene, isopentane, and ethylene on various types of biochar, including straw—sludge biochar, pure straw—sludge biochar, pure corn straw biochar, optimal straw—sludge biochar, and unactivated straw—sludge biochar, in 17 response surface tests. The results

indicate that the CO_2-activated modified straw—sludge biochar exhibits improved saturated adsorption capacity for methylbenzene, isopentane, and ethylene. Compared to unactivated straw—sludge biochar, the saturated adsorption capacity values of methylbenzene, isopentane, and ethylene by CO_2-activated straw—sludge biochar are 5.08−9.09, 6.74−9.72, and 7.64−10.76 times higher with the maximum adsorption capacities of 214.76 180.52, and 166.59 mg/g, respectively. The adsorption capacities of methylbenzene, isopentane, and ethylene differ among the biochar samples. Methylbenzene exhibits an adsorption capacity ranging from 120.03 to 214.04 mg/g, isopentane ranges from 125.24 to 182.05 mg/g, and ethylene

ranges from 118.31 to 166.59 mg/g. The adsorption order of VOCs in the 15 groups of biochar, from MAC-1 to MAC-13, MAC-15, and CAC, follows the sequence of methylbenzene > isopentane > ethylene. The methylbenzene adsorption capacity in the experimental group, MACM-1 to MACM-17, is 13.35−78.32% higher than that of pure sludge biochar (SAC) and 3.94−46.49% higher than that of pure corn straw biochar (CAC). Similarly, the adsorption capacity values of ACE-1 to ACE-17 in the experimental group are 5.91−41.18% higher than that of SAC and 2.11−31.48% higher than that of CAC. Furthermore, the ethylene adsorption capacity of MACI-1 to MACI-17 in the experimental group is 10.03−40.81% higher than that of SAC and 2.76−31.50% higher than that of CAC. The adsorption capacity of biochar for VOCs is closely related to the specific surface area. CO_2 activation of straw−sludge biochar enhances its adsorption efficiency for VOCs. The activation process facilitates the decomposition of impurities, resulting in an increased transparency of the pores and a larger specific surface area. These factors contribute to the improved saturated adsorption capacity of straw−sludge biochar for VOCs and enhance the utilization of waste straw−sludge biochar.[28]

3.2.4. Optimization of Preparation Conditions Based on Response Surface Methodology.

The raw material ratio, activation temperature, and activation time were set as influencing factors, and the adsorption amounts of methylbenzene, isopentane, and ethylene were set as response values. Based on this, the results were analyzed using Design Expert software, and the experimental results were fitted and significance tested. The relationships between the sorption of VOCs by straw−sludge biochar and the three independent variables (A), activation temperature (B), and activation time (C) are shown in eqs 5−7:

$$q_{e1} = 212.25 + 20.74A + 9.099B + 6.58C + 7.01AB$$
$$+ 1.17AC + 0.095BC - 33.59A^2 - 19.49B^2$$
$$- 10.42C^2 \tag{5}$$

$$q_{e2} = 180.17 + 14.37A + 5.68B + 3.87C - 0.96AB$$
$$+ 0.69AC - 0.37BC - 22.00A^2 - 10.24B^2$$
$$- 4.15C^2 \tag{6}$$

$$q_{e3} = 164.45 + 5.90A + 4.20B - 1.18C + 1.68AB$$
$$+ 4.13AC + 0.34BC - 15.30A^2 - 5.06B^2 - 6.49C^2 \tag{7}$$

The absolute value of the coefficients in the equation can reflect the effect of the term on the adsorption of VOCs. The positive sign indicates that there is a positive effect between the variable and dependent variable, the negative sign indicates that there is a negative effect between the two, and the content of the increasing factor can inhibit the adsorption. According to the above formula, the ratio of raw materials and activation temperature has great influence on VOC adsorption, but activation time has little effect on VOC adsorption. The proportion of raw materials, activation temperature, and activation time all have positive effects.

Table 5 shows that this model has a large correlation coefficient R^2, the residual sum of squares and the standard deviation are very small, C. V% <1.15% and adeq precisior above 26.499 indicated that the above three models could be

Table 5. Statistical Analysis of the Regression Equation Error

statistical items	value		
	methylbenzene	isopentane	ethylene
Std.Dev	1.98	1.87	1.62
mean	182.37	163.04	151.81
C.V%	1.08%	1.15%	1.07%
PRESS	295.05	285.21	145.06
R-squared	0.9977	0.9949	0.9903
adj R-squared	0.9948	0.9883	0.9779
pred R-square	0.9756	0.9405	0.9239
adeq precisior	50.103	37.032	26.499

used to describe the adsorption process of VOCs on straw−sludge biochar.

The optimal process conditions for the preparation of straw−sludge biochar preparation were optimized by using a Box-Behnken model, and the results are shown in Table 6. Based on the optimal conditions, mixed biochar was prepared, and subsequent adsorption experiments were performed. The experimental results aligned closely with the predicted values, with relative errors ranging from 0.75 to 2.41%. This indicates the reliability and suitability of the model for optimizing the straw−sludge biochar adsorption process for VOCs. The adsorption samples for methylbenzene, isopentane, and ethylene are named OACM-C, OACI-C, and OACE-C (obtained under the optimal process conditions), respectively. Based on this, subsequent action mechanics related analysis is carried out.

3.2.5. Adsorption Mechanism of VOCs on Straw−Sludge Biochar.

Figure 8 and Table 7 are quasi-first- and quasi-second-order kinetic curves and parameter values, which can be seen from R^2 >0.97, and the sorption of VOCs by straw−sludge biochar (OAC) and unactivated biochar (BC) accords with quasi-first-order and quasi-second-order kinetic models. The correlation coefficients fitted by the quasi-first-order kinetic model are higher than those fitted by the quasi-second-order kinetic model, and the theoretical adsorption capacity fitted by the quasi-first-order kinetic model is closer to the experimental value. The results show that the adsorption process of methylbenzene, isopentane, and ethylene on OAC accords with the quasi-first-order kinetic model controlled by physical diffusion. There are a lot of oxygen-containing functional groups on the surface of straw−sludge biochar prepared in the laboratory. The pore structure of straw−sludge biochar is very rich, the oxygen-containing functional groups on the surface disappear, and the electron-affinity decreases; the adsorption process is mainly controlled by diffusion.[22] In addition, the rate constant k_1 of OAC is larger than that of BC, so the adsorption rate of OAC is larger than that of BC; this is also in line with the results of the effect of adsorption time on the removal rate.[29]

The fitting results of isothermal adsorption are shown in Figure 9 and Table 8. The regression coefficient R^2 shows that the Freundlich model can describe the adsorption process of VOCs on BC; the Langmuir model can describe the adsorption of VOCs on the surface of OAC, which shows that the adsorption of VOCs on the surface of OAC is monolayer and restricted by the adsorption sites on the surface, which accords with the characteristics of chemical adsorption.[30]

Table 6. Optimum Process Conditions for Adsorption Capacity of VOCs by CO_2-Activated Straw−Sludge Biochar

adsorbate	raw material ratio	activation temperature (°C)	activation time (min)	predicted adsorption capacity (mg/g)	actual adsorption capacity (mg/g)	relative error (%)
methylbenzene	0.58	802.96	128.78	216.38	214.76	0.75
isopentane	0.63	808.89	122.30	182.29	185.72	1.85
ethylene	0.55	845.10	119.42	166.04	162.13	2.41
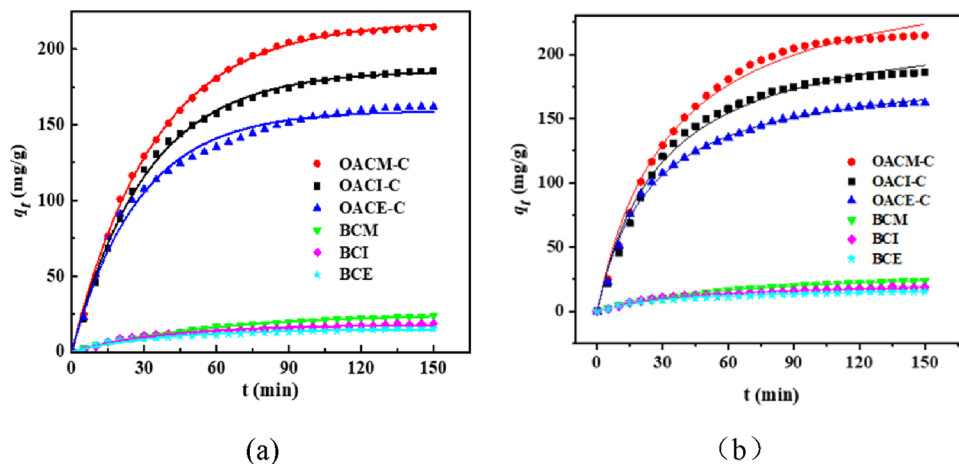
Figure 8. Kinetic curves of straw−sludge biochar: (a) quasi-first-order kinetic curves and (b) quasi-second-order kinetic curves.

Table 7. kinetic Parameters of Straw−Sludge Biochar

| adsorbent	quasi-second-order kinetic model			quasi-scond-order kinetic model		
	q_e (mg/g)	k_1	R^2	q_e (mg/g)	k_2	R^2
OACM-C	218.43	0.0295	0.9991	272.31	0.00011	0.9916
OACI-C	185.84	0.0325	0.9977	228.17	0.00015	0.9902
OACE-C	159.30	0.0361	0.9907	190.91	0.00022	0.9964
BCM	25.402	0.0170	0.9976	35.102	0.00040	0.9987
BCI	18.039	0.0256	0.9795	22.906	0.00111	0.9889
BCE	15.013	0.0270	0.9746	18.698	0.00152	0.9907
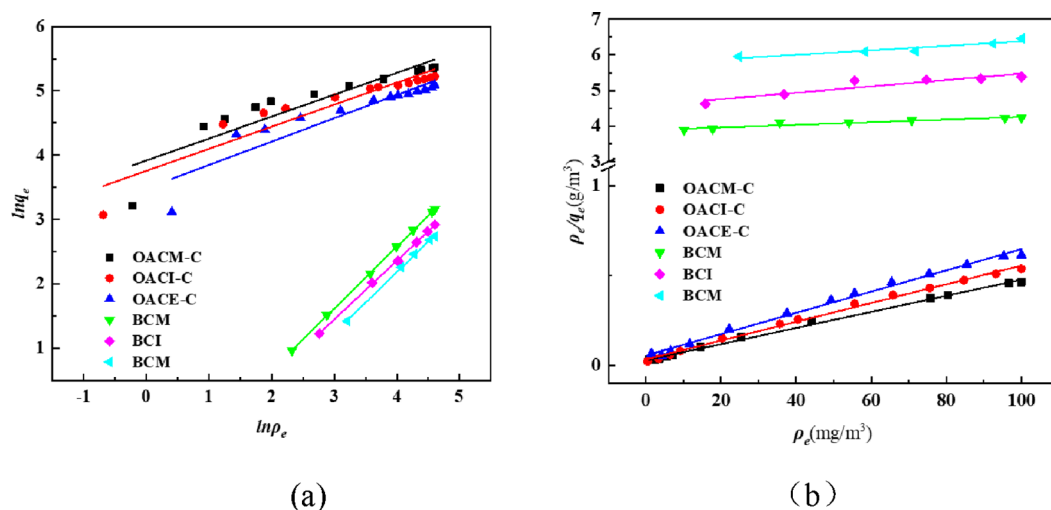
Figure 9. Isothermal adsorption curves of straw−sludge biochar: (a) Freundlich isothermal adsorption curve and (b) Langmuir isothermal adsorption curve.

In the Langmuir model, the k_L of the OAC is much larger than that of BC because the number of functional groups on the surface of BC is less than that of the OAC, and the chemical adsorption of the OAC is stronger. At the same time, the results also show that CO_2 activation can increase the specific surface area and pore volume of biochar, which is helpful to improve the adsorption of VOCs on Biochar. In the Freundlich model, the n values of the OAC were all greater than 1, which indicated that the mixed biochar was easy to adsorb VOCs. The higher the k_F value, the stronger the

Table 8. Isothermal Adsorption Parameters of Straw−Sludge Biochar

| adsorbent	Freundlich isothermal adsorption model			Langmuir isothermal adsorption model		
	k_F	n	R^2	q_m	k_L	R^2
OACM-C	50.4035	2.9376	0.8364	222.92	0.1511	0.9966
OACI-C	42.9029	2.9193	0.8850	191.31	0.1512	0.9957
OACE-C	32.6890	2.7556	0.8541	168.91	0.1045	0.9953
BCM	0.28197	1.0396	0.9999	25.102	0.0141	0.9811
BCI	0.27534	1.0951	0.9995	18.906	0.0255	0.9649
BCE	0.19924	1.0531	0.9991	15.698	0.0285	0.9580
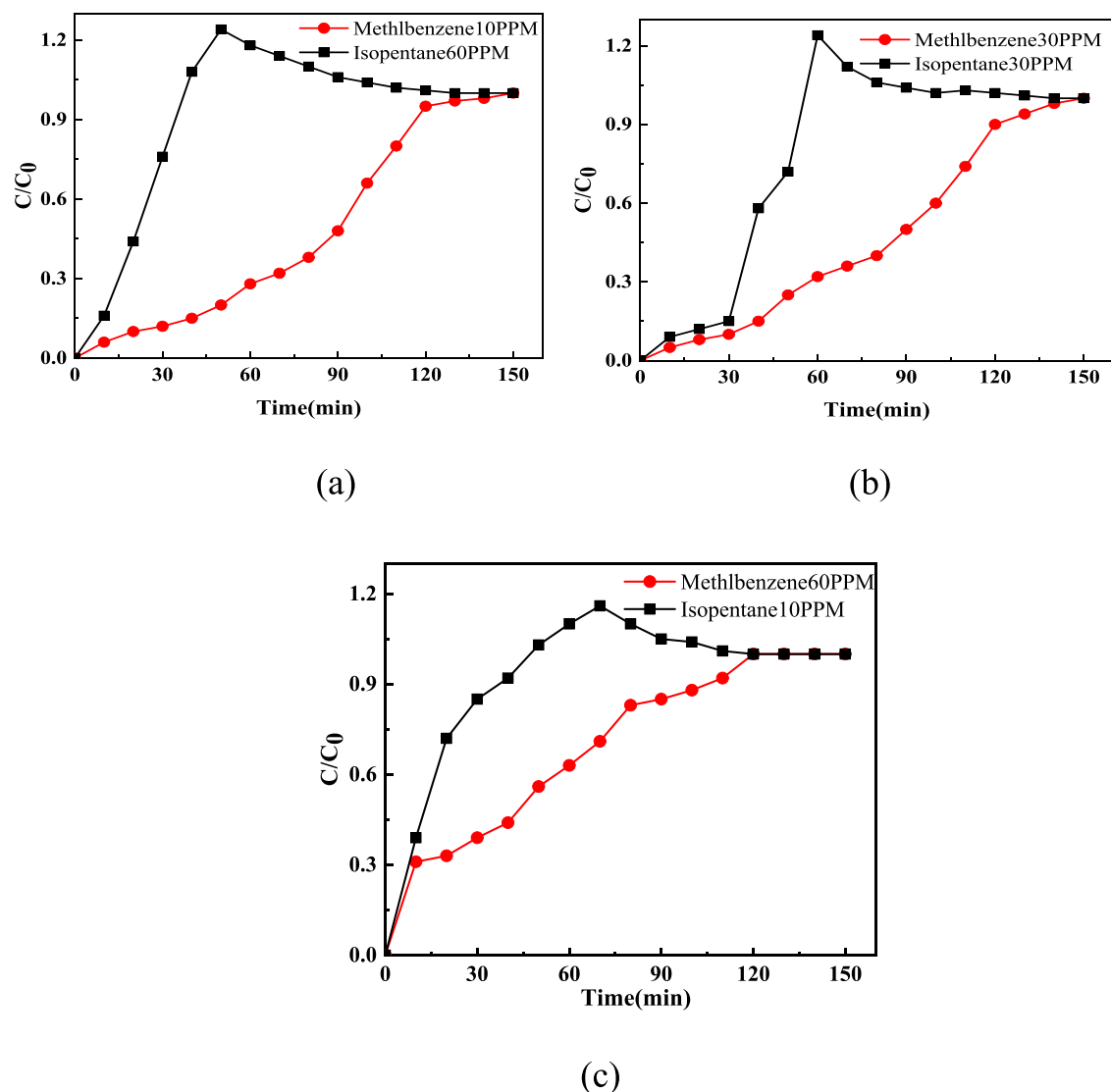
Figure 10. Competitive adsorption penetration curves of methylbenzene−isopentane at different initial concentrations on CO_2-activated straw−sludge biochar: (a) methylbenzene 10PPM−isopentane 60PPM, (b) methylbenzene 30PPM−isopentane 30PPM, and (c) methylbenzene 60PPM−isopentane 10PPM.

adsorption capacity. The k_F value of the OAC is much higher than that of BC, indicating that the biochar activated by CO_2 has a better adsorption capacity for VOCs.

3.2.6. Study on Binary Competitive Adsorption. To investigate competitive adsorption, we initially subjected the CO_2-activated straw−sludge biochar to individual adsorption experiments using methylbenzene, isopentane, and ethylene. From these experiments, the optimal group of biochar was selected based on response surface experiments. Subsequently, the same experimental setup and equipment were utilized to

conduct binary competitive adsorption experiments. These experiments focused on the interactions between methylbenzene−isopentane, methylbenzene−ethylene, and isopentane−ethylene at different inlet concentrations: 10 PPM/60 PPM, 30 PPM/30 PPM, and 60 PPM/10 PPM, respectively.

The competitive adsorption results depicted in Figure 10 reveal a common trend among the three different ratios of methylbenzene−isopentane. In the presence of methylbenzene as a competitor, isopentane consistently exhibits higher export concentrations compared to its input concentrations, even
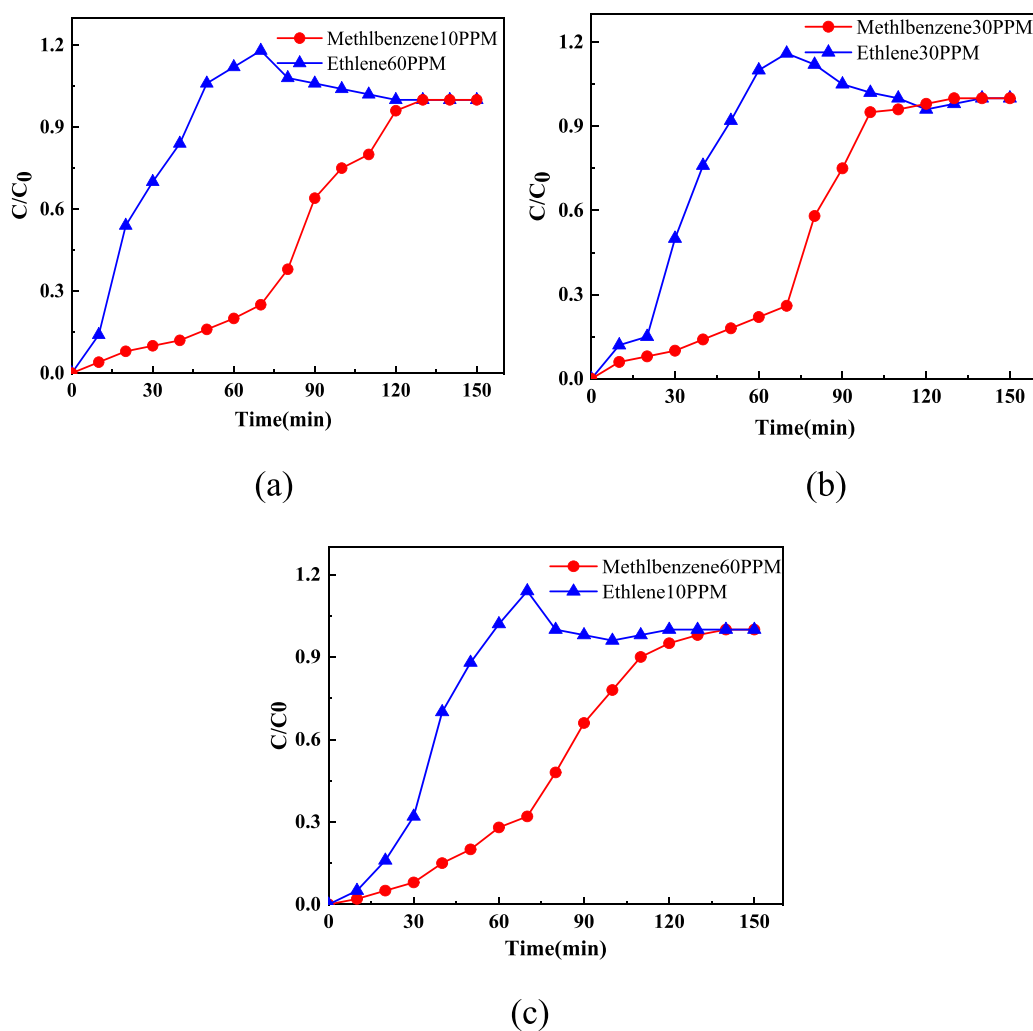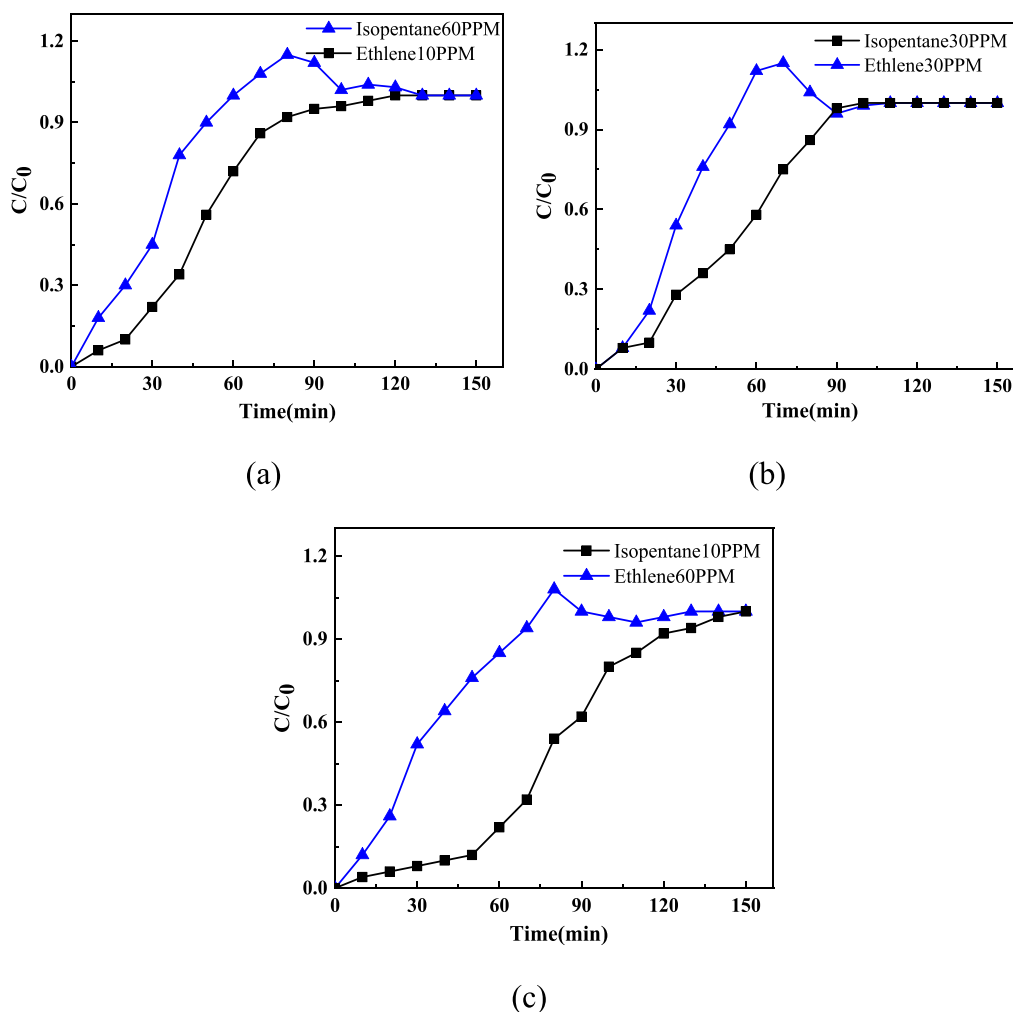
Figure 11. Competitive adsorption penetration curves of methylbenzene−ethylene at different initial concentrations on CO_2-activated straw−sludge biochar: (a) methylbenzene 10PPM−ethylene 60PPM, (b) methylbenzene 30PPM−ethylene 30PPM, and (c) methylbenzene 60PPM−ethylene 10PPM.

when the isopentane concentration is only 1/6th of the methylbenzene concentration, resulting in a peak effect. This phenomenon arises from the fact that methylbenzene, possessing the same polarity as straw−sludge biochar, gains a distinct advantage in competition with isopentane, resulting in a higher adsorption rate. Furthermore, even after the adsorption of methylbenzene reaches equilibrium, a portion of the isopentane adsorbed by the straw−sludge biochar can be displaced, leading to the desorption of isopentane.[31] Moreover, the duration and shape of these three peaks differ across the three concentration ratios. The peak shape is determined by the combined properties of the straw−sludge biochar and VOCs. Factors such as pore size primarily impact straw−sludge biochar, while the molecular kinetic diameter, molecular polarity, and concentration play a more significant role in VOCs. Additionally, when compared with the adsorption processes of methylbenzene and isopentane individually, the linearity and adsorption capacity remain quite similar. This indicates that the pore size of straw−sludge biochar is a critical factor determining both the adsorption capacity and results.

Figure 11 displays the competitive adsorption penetration curves of methylbenzene−ethylene at various initial concentrations on CO_2-activated straw−sludge biochar. Initially, the

adsorption process of methylbenzene−ethylene resembles that of individual adsorption, with both curves exhibiting an upward trend due to the absence of the competitive adsorption interference between the molecules. As the adsorption time increases, ethylene enters the replacement stage, leading to a steeper slope in the adsorption curve. However, when the outlet concentration reaches the inlet concentration, the concentration continues to rise, exceeding the inlet concentration by 20%. Notably, an evident "hump" phenomenon appears in the adsorption curve. During the initial adsorption stage, an ample number of adsorption sites on the CO_2-activated straw−sludge biochar are available to accommodate both methylbenzene and ethylene. As the adsorption sites gradually become occupied, methylbenzene gas molecules displace ethylene molecules with weaker adsorption capabilities. Consequently, the adsorbed ethylene molecules in the mesoporous channels and on the mesoporous surfaces desorb, resulting in an increase in the gas concentration of one component at the exit, surpassing that at the entrance. The pore size of the biochar used in the experiment is 2−4 nm, and the dominant factors influencing adsorption are not solely the molecular diameter of the adsorbate but also the polarity index, boiling point, molecular weight, and other related factors.[32]

Figure 12. Competitive adsorption penetration curves of different initial concentrations of isopentane−ethylene on CO_2-activated straw−sludge biochar: (a) isopentane 10PPM−ethylene 60PPM, (b) isopentane 30PPM−ethylene 30PPM, and (c) isopentane 60PPM−ethylene 10PPM.

Figure 12 illustrates the competitive adsorption penetration curves for different initial concentrations of isopentane−ethylene on the CO_2-activated straw−sludge biochar. Initially, both isopentane and ethylene can freely adsorb onto the surface of the biochar, as a significant number of active adsorption sites remain unsaturated. As the available adsorption sites on the CO_2-activated straw−sludge biochar surface decrease, a competition for adsorption occurs between isopentane and ethylene molecules, leading to the substitution stage. Ethylene demonstrates earlier penetration and approaches adsorption saturation in the biochar. However, isopentane displaces the previously adsorbed ethylene in the mesopores due to its higher polarity index. Upon reaching saturation, the CO_2-activated straw−sludge biochar begins absorbing isopentane, and the ethylene curve approaches equilibrium. Adsorption ceases when the outlet concentration equals the inlet concentration.

Based on the experimental results, it can be concluded that the adsorption capacity of the tested VOCs on CO_2-activated straw−sludge biochar follows the order of methylbenzene > isopentane > ethylene, which aligns with the boiling point order of the three organic compounds. This corresponding relationship may possess some correlation. During the adsorption process, exothermic reactions occur, leading to an increase in the temperature of the adsorption column and a

reduction in the equilibrium adsorption capacity of the CO_2-activated straw−sludge biochar. Since the adsorption experiment is conducted at room temperature, lower boiling point organic compounds are more susceptible to temperature effects, resulting in a rapid reduction in their adhesion to straw−sludge biochar due to the influence of adsorption heat. Conversely, high boiling point organic compounds exhibit minimal effects.

As exothermic heat accumulates throughout the adsorption process, lower boiling point compounds experience reduced adhesion to straw−sludge biochar, leading to gradual desorption reactions. On the other hand, higher boiling point compounds occupy more vacant spaces within the adsorbent. This phenomenon is observed in the competitive adsorption curve, where stronger adsorbates replace weaker adsorbates, resulting in a "bulge" on the adsorption penetration curve for weak adsorbates. Additionally, VOCs with higher molecular weights exhibit lower desorption rates with CO_2-activated straw−sludge biochar under the influence of adsorption heat. Conversely, organic compounds with lower molecular weights are more susceptible to adsorption heat, leading to their nonadsorption and subsequent dispersion in the gas stream.

Table 9. Comparison of the Adsorption Effects of Biochar on VOCs

adsorbent	activation method	adsorbate	adsorption effect	references
wheat straw-bagasse biochar	no	acetone/hexane/methylbenzene	51−110 mg/g	(33)
bone biochar	HNO_3	methylbenzene	288.12 mg/g	(34)
sawdust biochar	ammonia	dichlorotoluene	585 mg/g	(35)
	$KHCO_3$ and $NaHCO_3$	methane/methylbenzene	54.9/308 mg/g	(36)
straw biochar	CO_2	methylbenzene/hexane	81.7/60.6 mg/g	(37)
	H_2O	hexane	54.8 mg/g	(37)
commercial biochar		methylbenzene/hexane/butane	86/101.3 mg/g	(37)
barley hull biochar	50%H_2O + 0%N_2	benzene	227 mg/g	(38)
straw−sludge biochar	CO_2	methylbenzene/isopentane/ethylene	216.38 mg/g/182.29 mg/g/166.04 mg/g	this study

4. CONCLUSIONS

The adsorption capacity of straw−sludge biochar for VOCs followed a specific pattern: optimal group (OAC) > response surface group (MAC) > single raw material group (SAC/ CAC) > unactivated group (BC). Within the same sample, the adsorption capacity ranked as methylbenzene > isopentane > ethylene. The maximum saturated adsorption capacities of Mac for methylbenzene, isopentane, and ethylene was 9.09, 10, and 10.47 times higher than that of BC, respectively. They were 78.32, 40.81, and 41.18% higher than the SAC group, respectively. Compared with the CAC Group, they were increased by 46.49, 31.50, and 31.48% respectively. The adsorption process of VOCs by sludge-based biochar is controlled by physical diffusion, and the adsorption process is closer to monolayer adsorption. The sorption capacity of VOCs on straw−sludge biochar was methylbenzene > isopentane > ethylene.

At present, biochar prepared from biomass has been reported as a potential adsorbent for VOCs. There are many types of common biochar adsorbents, including nonactivated biochar, physically activated biochar (activator is CO_2 or H_2O), chemically modified biochar (activator is acid or alkali), and heteroatom loaded modified biochar. The adsorption effects of various types of biochar are shown in Table 9. It is found that the adsorption effect of biochar modified with acid, alkali, or inorganic salts on VOCs is significantly better than that of physically activated biochar. However, the production cost of this type of biochar is high and it has certain environmental pollution. The activated biochar produced by CO_2 or H_2O has various advantages: low production cost, simple operation process, and more environmentally friendly. Compared with the unactivated biochar, its adsorption effect is greatly improved, and its adsorption effect will be increased by 5−10 times.; The preparation process has the characteristics of low cost and environmental protection. Compared with commercial charcoal, its adsorption effect can reach 1−2 times that of commercial biochar. Taking the straw−sludge biochar prepared in this study as an example, its adsorption capacity for toluene is 5.1 times that of activated biochar and 3.2 times that of commercial biochar.[33−38]

■ AUTHOR INFORMATION

Corresponding Author

Youzhou Jiao − Key Laboratory of New Materials and Facilities for Rural Renewable Energy of Ministry of Agriculture and Rural Affairs, College of Mechanical & Electrical Engineering, Henan International Joint Laboratory of Biomass Energy and Nanomaterials, and Henan Collaborative Innovation Center of Biomass Energy, Henan Agricultural University, Zhengzhou 450002, China; Email: jiaoyouzhou@126.com

Authors

Xiaohui Pan − Key Laboratory of New Materials and Facilities for Rural Renewable Energy of Ministry of Agriculture and Rural Affairs, College of Mechanical & Electrical Engineering, Henan International Joint Laboratory of Biomass Energy and Nanomaterials, and Henan Collaborative Innovation Center of Biomass Energy, Henan Agricultural University, Zhengzhou 450002, China; ◉ orcid.org/0000-0002-9001-1728

Ninglu Zhang − Key Laboratory of New Materials and Facilities for Rural Renewable Energy of Ministry of Agriculture and Rural Affairs, College of Mechanical & Electrical Engineering, Henan International Joint Laboratory of Biomass Energy and Nanomaterials, and Henan Collaborative Innovation Center of Biomass Energy, Henan Agricultural University, Zhengzhou 450002, China

Le Yang − Key Laboratory of New Materials and Facilities for Rural Renewable Energy of Ministry of Agriculture and Rural Affairs, College of Mechanical & Electrical Engineering, Henan International Joint Laboratory of Biomass Energy and Nanomaterials, and Henan Collaborative Innovation Center of Biomass Energy, Henan Agricultural University, Zhengzhou 450002, China

Chao He − Key Laboratory of New Materials and Facilities for Rural Renewable Energy of Ministry of Agriculture and Rural Affairs, College of Mechanical & Electrical Engineering, Henan International Joint Laboratory of Biomass Energy and Nanomaterials, and Henan Collaborative Innovation Center of Biomass Energy, Henan Agricultural University, Zhengzhou 450002, China

Xiaoran Ma − Key Laboratory of New Materials and Facilities for Rural Renewable Energy of Ministry of Agriculture and Rural Affairs, College of Mechanical & Electrical Engineering, Henan International Joint Laboratory of Biomass Energy and Nanomaterials, and Henan Collaborative Innovation Center of Biomass Energy, Henan Agricultural University, Zhengzhou 450002, China

Xinxin Liu − Key Laboratory of New Materials and Facilities for Rural Renewable Energy of Ministry of Agriculture and Rural Affairs, College of Mechanical & Electrical Engineering, Henan International Joint Laboratory of Biomass Energy and Nanomaterials, and Henan Collaborative Innovation Center of Biomass Energy, Henan Agricultural University, Zhengzhou 450002, China

Liang Liu − Key Laboratory of New Materials and Facilities for Rural Renewable Energy of Ministry of Agriculture and Rural Affairs, College of Mechanical & Electrical Engineering,

Henan International Joint Laboratory of Biomass Energy and Nanomaterials, and Henan Collaborative Innovation Center of Biomass Energy, Henan Agricultural University, Zhengzhou 450002, China

Tingting Hou − *Key Laboratory of New Materials and Facilities for Rural Renewable Energy of Ministry of Agriculture and Rural Affairs, College of Mechanical & Electrical Engineering, Henan International Joint Laboratory of Biomass Energy and Nanomaterials, and Henan Collaborative Innovation Center of Biomass Energy, Henan Agricultural University, Zhengzhou 450002, China*

Complete contact information is available at:
https://pubs.acs.org/10.1021/acsomega.3c04866

Notes
The authors declare no competing financial interest.

■ REFERENCES

(1) Gyamfi, B. A.; Ozturk, I.; Bein, M. A.; Bekun, F. V. An investigation into the anthropogenic effect of biomass energy utilization and economic sustainability on environmental degradation in E7 economies. *Biofuels, Bioprod. Biorefin.* **2021**, *15* (3), 840−851.

(2) Mian, M. M.; Liu, G.; Zhou, H. Preparation of N-doped biochar from sewage sludge and melamine for peroxymonosulfate activation: N-functionality and catalytic mechanisms. *Sci. Total Environ.* **2020**, *744*, No. 140862.

(3) Qiu, Z.; Zhai, Y.; Li, S.; Liu, X.; Liu, X.; Wang, B.; Liu, Y.; Li, C.; Hu, Y. Catalytic co-pyrolysis of sewage sludge and rice husk over biochar catalyst: Bio-oil upgrading and catalytic mechanism. *Waste Manage.* **2020**, *114*, 225−233.

(4) Tong, S.; Zhang, S.; Yin, H.; Wang, J.; Chen, M. Study on co-hydrothermal treatment combined with pyrolysis of rice straw/sewage sludge: Biochar properties and heavy metals behavior. *J. Anal. Appl. Pyrolysis* **2021**, *155*, No. 105074.

(5) Xing, J.; Xu, G.; Li, G. Comparison of pyrolysis process, various fractions and potential soil applications between sewage sludge-based biochars and lignocellulose-based biochars. *Ecotoxicol. Environ. Saf.* **2021**, *208*, No. 111756.

(6) Qin, Z.; Lei, M.; Zhang, L. Thermogravimetric analysis of the co-combustion of bituminous coal,rice straw and sewage sludge. *IOP Conf. Ser.: Earth Environ. Sci.* **2022**, *1011* (1), No. 012028.

(7) Li, B.; Ho, S. S. H.; Li, X.; Guo, L.; Chen, A.; Hu, L.; Yang, Y.; Chen, D.; Lin, A.; Fang, X. A comprehensive review on anthropogenic volatile organic compounds (VOCs) emission estimates in China: Comparison and outlook. *Environ. Int.* **2021**, *156*, No. 106710.

(8) Liu, B.; Ji, J.; Zhang, B.; Huang, W.; Gan, Y.; Leung, D. Y. C.; Huang, H. Catalytic ozonation of VOCs at low temperature: A comprehensive review. *J. Hazard. Mater.* **2022**, *422*, No. 126847.

(9) Wu, C.; Zhang, C.; Bai, L. Characteristics of Volatile Organic Compounds Emitted from Biomass-Pellets Fired Boilers. *Environmental Science* **2017**, *38* (6), 2238−2245.

(10) Zhu, J.; Li, Y.; Xu, L.; Liu, Z. Removal of toluene from waste gas by adsorption-desorption process using corncob-based activated carbons as adsorbents. *Ecotoxicol. Environ. Saf.* **2018**, *165*, 115−125.

(11) Danish, M.; Ahmad, T. A review on utilization of wood biomass as a sustainable precursor for activated carbon production and application. *Renewable Sustainable Energy Rev.* **2018**, *87*, 1−21.

(12) Igalavithana, A. D.; Mandal, S.; Niazi, N. K.; Vithanage, M.; Parikh, S. J.; Mukome, F. N. D.; Rizwan, M.; Oleszczuk, P.; Al-Wabel,

M.; Bolan, N.; et al. Advances and future directions of biochar characterization methods and applications. *Crit. Rev. Environ. Sci. Technol.* **2017**, *47* (23), 2275−2330.

(13) Qian, K.; Kumar, A.; Zhang, H.; Bellmer, D.; Huhnke, R. Recent advances in utilization of biochar. *Renewable Sustainable Energy Rev.* **2015**, *42*, 1055−1064.

(14) Zhang, Z.; Jiang, C.; Li, D.; Lei, Y.; Yao, H.; Zhou, G.; Wang, K.; Rao, Y.; Liu, W.; Xu, C.; et al. Micro-mesoporous activated carbon simultaneously possessing large surface area and ultra-high pore volume for efficiently adsorbing various VOCs. *Carbon* **2020**, *170*, 567−579.

(15) Ukalska-Jaruga, A.; Smreczak, B.; Klimkowicz-Pawlas, A. Soil organic matter composition as a factor affecting the accumulation of polycyclic aromatic hydrocarbons. *J. Soils Sed.* **2019**, *19* (4), 1890−1900.

(16) Akinpelu, A. A.; Ali, M. E.; Johan, M. R.; Saidur, R.; Qurban, M. A.; Saleh, T. A. Polycyclic aromatic hydrocarbons extraction and removal from wastewater by carbon nanotubes: A review of the current technologies, challenges and prospects. *Process Saf. Environ. Prot.* **2019**, *122*, 68−82.

(17) Khan, A.; Szulejko, J. E.; Samaddar, P.; Kim, K.-H.; Liu, B.; Maitlo, H. A.; Yang, X.; Ok, Y. S. The potential of biochar as sorptive media for removal of hazardous benzene in air. *Chem. Eng. J.* **2019**, *361*, 1576−1585.

(18) Zhang, X.; Xiang, W.; Wang, B.; Fang, J.; Zou, W.; He, F.; Li, Y.; Tsang, D. C. W.; Ok, Y. S.; Gao, B. Adsorption of acetone and cyclohexane onto CO2 activated hydrochars. *Chemosphere* **2020**, *245*, No. 125664.

(19) Shih, Y.-h.; Li, M.-s. Adsorption of selected volatile organic vapors on multiwall carbon nanotubes. *J. Hazard. Mater.* **2008**, *154* (1), 21−28.

(20) Yang, X.; Yi, H.; Tang, X.; Zhao, S.; Yang, Z.; Ma, Y.; Feng, T.; Cui, X. Behaviors and kinetics of toluene adsorption-desorption on activated carbons with varying pore structure. *JEnvS* **2018**, *67*, 104−114.

(21) Hou, B.; Zhao, Y.; Sun, W.; Lu, S.; Chen, S. Glycine based modification of activated carbons for VOCs adsorption. *Chem. Eng. J. Adv.* **2021**, *7*, No. 100126.

(22) Sánchez-Monedero, M. A.; Sánchez-García, M.; Alburquerque, J. A.; Cayuela, M. L. Biochar reduces volatile organic compounds generated during chicken manure composting. *Bioresour. Technol.* **2019**, *288*, No. 121584.

(23) Behera, S. K.; Meena, H.; Chakraborty, S.; Meikap, B. C. Application of response surface methodology (RSM) for optimization of leaching parameters for ash reduction from low-grade coal. *Int. J. Min. Sci. Technol.* **2018**, *28* (4), 621−629.

(24) Wang, J.; Guo, X. Adsorption kinetic models: Physical meanings, applications, and solving methods. *J. Hazard. Mater.* **2020**, *390*, No. 122156.

(25) Ezzati, R. Derivation of Pseudo-First-Order, Pseudo-Second-Order and Modified Pseudo-First-Order rate equations from Langmuir and Freundlich isotherms for adsorption. *Chem. Eng. J.* **2020**, *392*, No. 123705.

(26) Jing, J.; Li, L.; Chu, W.; Wei, Y.; Jiang, C. Microwave-assisted synthesis of high performance copper-based catalysts for hydrogen production from methanol decomposition. *Int. J. Hydrogen Energy* **2018**, *43* (27), 12059−12068.

(27) Chu, K. H. Breakthrough curve analysis by simplistic models of fixed bed adsorption: In defense of the century-old Bohart-Adams model. *Chem. Eng. J.* **2020**, *380*, No. 122513.

(28) Meng, F.; Song, M.; Wei, Y.; Wang, Y. The contribution of oxygen-containing functional groups to the gas-phase adsorption of volatile organic compounds with different polarities onto lignin-derived activated carbon fibers. *Environ. Sci. Pollut. Res.* **2019**, *26* (7), 7195−7204.

(29) Hassan, M.; Liu, Y.; Naidu, R.; Parikh, S. J.; Du, J.; Qi, F.; Willett, I. R. Influences of feedstock sources and pyrolysis temperature on the properties of biochar and functionality as adsorbents: A meta-analysis. *Sci. Total Environ.* **2020**, *744*, No. 140714.

(30) Xiang, W.; Zhang, X.; Chen, K.; Fang, J.; He, F.; Hu, X.; Tsang, D. C. W.; Ok, Y. S.; Gao, B. Enhanced adsorption performance and governing mechanisms of ball-milled biochar for the removal of volatile organic compounds (VOCs). *Chem. Eng. J.* **2020**, *385*, No. 123842.

(31) Li, X.; Wang, C.; Zhang, J.; Liu, J.; Liu, B.; Chen, G. Preparation and application of magnetic biochar in water treatment: A critical review. *Sci. Total Environ.* **2020**, *711*, No. 134847.

(32) Cheng, N.; Wang, B.; Wu, P.; Lee, X.; Xing, Y.; Chen, M.; Gao, B. Adsorption of emerging contaminants from water and wastewater by modified biochar: A review. *Environ. Pollut.* **2021**, *273*, No. 116448.

(33) Rajabi, H.; Hadi Mosleh, M.; Prakoso, T.; Ghaemi, N.; Mandal, P.; Lea-Langton, A.; Sedighi, M. Competitive adsorption of multicomponent volatile organic compounds on biochar. *Chemosphere* **2021**, *283*, No. 131288.

(34) Yang, Y.; Sun, C.; Huang, Q.; Yan, J. Hierarchical porous structure formation mechanism in food waste component derived N-doped biochar: Application in VOCs removal. *Chemosphere* **2022**, *291*, No. 132702.

(35) Pi, X.; Qu, Z.; Sun, F.; Zhang, Z.; Gao, J. Catalytic activation preparation of nitrogen-doped hierarchical porous bio-char for efficient adsorption of dichloromethane and toluene. *J. Anal. Appl. Pyrolysis* **2021**, *156*, No. 105150.

(36) Liu, S.; Peng, Y.; Chen, J.; Yan, T.; Zhang, Y.; Liu, J.; Li, J. A new insight into adsorption state and mechanism of adsorbates in porous materials. *J. Hazard. Mater.* **2020**, *382*, No. 121103.

(37) Zhang, Z.; Ning, S.; Li, Q.; Sun, M.; Lin, J.; Wang, X. Levels and risk assessment of polycyclic aromatic hydrocarbons in wood vinegars from pyrolysis of biomass. *Chemosphere* **2021**, *278*, No. 130453.

(38) Hsi, H.-C.; Horng, R. S.; Pan, T.-A.; Lee, S.-K. Preparation of Activated Carbons from Raw and Biotreated Agricultural Residues for Removal of Volatile Organic Compounds. *J. Air Waste Manage. Assoc.* **2011**, *61* (5), 543−551.